

Learning and Transferring Value Function for Robot Exploration in Subterranean Environments

Yafei Hu^{1,2}, Chen Wang¹, John Keller¹ and Sebastian Scherer^{1,2}

Abstract—In traditional robot exploration methods, the robot usually does not have prior biases about the environment it is exploring. Thus the robot assigns equal importance to the goals which leads to insufficient exploration efficiency. Alternative, often a hand-tuned policy is used to tweak the value of goals. In this paper, we present a method to learn how “good” some states are, measured by the state value function, to provide a hint for the robot to make exploration decisions. We propose to learn state value functions from previous offline collected datasets and then transfer and improve the value function during testing in a new environment. Moreover, the environments usually have very few and even no extrinsic reward or feedback for the robot. Therefore in this work, we also tackle the problem of sparse extrinsic rewards from the environments. We design several intrinsic rewards to encourage the robot to obtain more information during exploration. These reward functions then become the building blocks of the state value functions. We test our method on challenging subterranean and urban environments. To the best of our knowledge, this work for the first time demonstrates value function prediction with previous collected datasets to help exploration in challenging subterranean environments.

I. INTRODUCTION

In conventional robot exploration, robots usually do not know whether a certain state is worthy of exploring. Conventional methods such as information gain-based and frontier-based exploration select exploration goals by maximizing the information gain [1] or unexplored frontiers [2]. The actions are then obtained from some heuristic graph search algorithms such as A* or Rapidly-exploring Random Tree (RRT). These conventional methods, however, fail to prioritize more important states/regions which have higher value to explore.

More recently, inspired by the exploration-exploitation trade-off and intelligent exploration [3] [4] [5] [6] in reinforcement learning (RL), RL based approaches were used on robot exploration [7] [8]. In these methods, the value functions are learned from the experience sampled from the online interactions with the environment. However, collecting large amount of data via online interaction with the environment is inappropriate for real-world robotic applications. Thus, offline RL is applied to tackle this problem [9] [10] by learning policy/value function via previous collected data. Moreover, in these methods, the robot treats the environments as completely novel and no prior knowledge about the environment is applied when exploring the new environment, hence treating the robots as tabula-rasa agents [11].

To solve this problem, we propose a state value function learner with previous collected data. Similar to the prediction

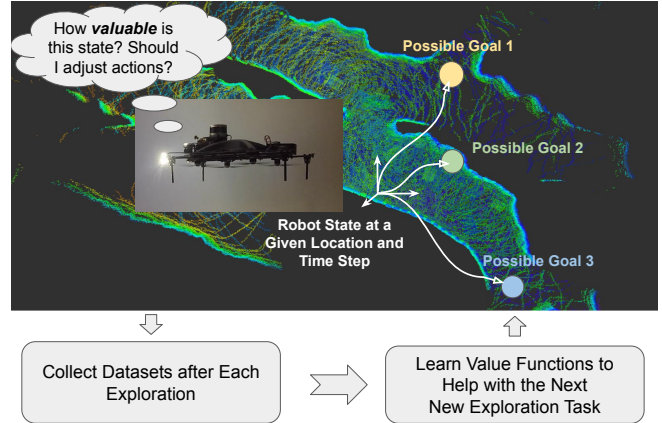


Fig. 1: Background of the proposed value function learning and transferring: The robot explores new environments with a given policy and needs to decide how good/valuable the next possible goals are. To learn a reasonable state value function, we use prior data which contains the trajectories and the rewards a robot receives during the previous explorations. These data will then be used to train an offline value function approximator and then if deployed in a similar environment it may help the robot make decisions and adjust exploration policy to explore states with higher accumulated reward.

problems introduced in offline RL [9], we train the value function approximator offline and then deploy the predicted value function online to help with the robot exploration. During online deployment, we also exploit the recursive property of value function and propose an online learning scheme to improve the value function estimation in testing stage. In addition, to alleviate the problem of overestimation of value function [12] [10], we propose to use a double value network structure.

Apart from the state value prediction during exploration, in many scenarios, the extrinsic rewards from the environment could be sparse and even non-existent. This is also known as the hard exploration problem in RL [7]. Several intrinsic rewards were proposed such as visitation count [5], curiosity [13] [4] and etc. However, the state representation in these methods largely rely on image frames from the environments. Moreover, these methods are often tested in non-robotic environments instead of challenging real-world environments. The environment where our datasets are collected are several subterranean and urban environments such as abandoned urban building with rooms and corridors, underground mining bends and natural caves. The major challenges of these environments are that they are extremely unstructured, they provide sparse extrinsic rewards for the

¹Robotics Institute, Carnegie Mellon University

²Electrical and Computer Engineering, Carnegie Mellon University

agents, the environments are procedurally-generated. Like previous introduced methods based on intrinsic rewards, we also proposed several intrinsic rewards to encourage the robots to acquire richer information about the environment. These information are obtained from various sensors such as on-board camera, Lidar and etc. Thus our intrinsic rewards have a much richer representation of the real world comparing with aforementioned approaches which mainly reply on images from the simulation.

In summary, in this paper our contributions can be mainly summarized as following:

- We proposed several intrinsic rewards which help the robot acquire more information given sparse extrinsic rewards from the environments.
- We train the value function with prior batch data.
- We use a Temporal Difference (TD) learning scheme to optimize the offline trained value estimator.
- We use double value networks to mitigate the problem of overestimation of value function.

II. RELATED WORK

One of the early exploration methods is information gain-based exploration [14]. Information gain-based exploration typically use greedy strategy [1] [15], which greedily choose actions which maximize the information gain. Another perspective to solve the exploration problem is frontier-based exploration [2] [16]. Frontiers are typically defined as some selected points in the boundary between explored and unexplored areas. [2] use a 2D occupancy grid map and detect frontier points by clustering the frontier edge segments. Some more recent works such as [16] uses 3D occupancy grid map and a more efficient frontier selection method in frontier-based exploration. More recently, next-best-view approaches [17] randomly select unexplored areas instead of just selecting goals from the frontiers. This randomness could help the robot gather more information.

The exploration actions from these traditional exploration methods are less versatile for different environments and exploration tasks. Thus some reinforcement learning (RL) methods could help alleviating this problem. RL-based methods can improve the policy and value function through the interaction with the environment. Conventional RL exploration techniques such as ϵ -greedy and Upper Confidence Bound (UCB) take care of the exploitation and exploration trade-off by not only greedily picking actions with highest action value but also picking random or less used actions.

More Recently, some more intelligent exploration methods were proposed, such as visitation count based [5], curiosity-based [4], memory based [18] and etc. [5] [19] [20] use state visitation count as intrinsic reward for exploration. Due to high-dimensional continual state space, [5] [19] use a state pseudo-count model derived from Context-Tree Switching density model. Besides count-based exploration, curiosity-based intrinsic rewards [13] [4] were proposed to encourage agents to visited “unexpected” states which have higher prediction error. [7] and [11] use changes of states as the intrinsic reward to encourage agents to learn policy

which may have higher impact. [11] proposed interest-based transferring for exploration but this method is only tested in well-structured simulation environment.

These intelligent exploration algorithms require large amount of sample to train the policy and value function in an online manner. Thus it is impractical to deploy these algorithms in real robot considering time and other costs. Thus more recently, offline reinforcement learning [9] [10] algorithms are used to train the policy and value function offline and then transfer them online to a new environment. Similar to offline reinforcement learning, we also use previous collected data to learn the value function given a policy and then deploy the value function prediction online to help the robot select states with high accumulated rewards.

III. PROBLEM FORMULATION

The exploration procedure is formulated as a Markov Decision Process (MDP) defined by the tuple $(\mathcal{S}, \mathcal{A}, \mathcal{R}, \mathcal{P}, \gamma)$. $\mathcal{S} \in \mathbb{R}^m$ represents the state space. $\mathcal{A} \in \mathbb{R}^n$ denotes the action space. $\mathcal{R} : \mathcal{S} \times \mathcal{A} \rightarrow \mathbb{R}$ is the reward space, $\mathcal{P} : \mathcal{S} \times \mathcal{A} \times \mathcal{S} \rightarrow \mathbb{R}_+$ denotes the stochastic state transition dynamic model, e.g., at time t , $p(s_{t+1}|s_t, a_t) \in \mathcal{P}$. $\gamma \in [0, 1]$ denotes the discounting factor. We also define policy $\pi : \mathcal{S} \times \mathcal{A} \rightarrow \mathbb{R}_+$ which is a mapping from state to action. The robot exploration trajectory ξ is thus a tuple $\{s_0, a_0, r_0, \dots, s_{T-1}, a_{T-1}, r_{T-1}\}$ following the MDP, with $s \in \mathcal{S}$, $a \in \mathcal{A}$, $r \in \mathcal{R}$. Here T denotes the horizon of one exploration episode. The data we use to learn the value function is a collection of trajectories, $\mathcal{D} = \{\xi_1, \xi_2, \dots, \xi_M\}$. Different from the RL based exploration methods, the exploration policy is based on the frontier-based exploration shown in [2] [21].

We formulate our value function approximation problem as a prediction problem given an exploration policy $\pi(a|s)$. Our goal is to learn state value function $\hat{V}(\phi(s_t))$, $\forall s \in \mathcal{S}$ which approximate the truth value function $V_\pi(s_t)$ following the exploration policy $\pi(a|s)$ and then try to generalize and improve the value function in testing environments. Here $\phi(s_t)$ denotes the representation of state at time step t . We will use images captured from the on-board camera and the occupancy grid map to represent the states.

Although it is straightforward to formulate this environment as a tabular grid world and solve the value function $V_\pi(s)$ with dynamic programming based prediction approach such as policy evaluation [22], the robot that is used to explore the environments where data is collected is equipped with multiple sensors and more information beyond the locations of the robot are taken into consideration when formulating the representations of the robot’s state. For example, we will consider the visual coverage from the on-board camera as one of the representations of the robot’s state. Thus, the state space \mathcal{S} is actually continuous and we will be using a function approximator to learn the state value function $V_\pi(s)$. The state transition $p(s_{t+1}|s_t, a_t)$ is also unknown since the structure of the environment won’t be fully revealed before fully exploring the environment.

IV. METHOD

A. Exploration Policy

During exploration, we maintain two sets of map: 1) frontier map which contains regions which are not explored yet, and 2) camera observed map which contains the regions within the frustum of the on-board camera for object detection. Both frontier and camera observed map are represented as the 3D occupancy grid map. The robot also search for interesting objects such as backpacks, cellphones and etc, which may serve as signals for search and rescue. We may use these object information as reward in exploration, however the interesting objects are often sparse in the environments. The 3D map representation is shown in Fig. 2.

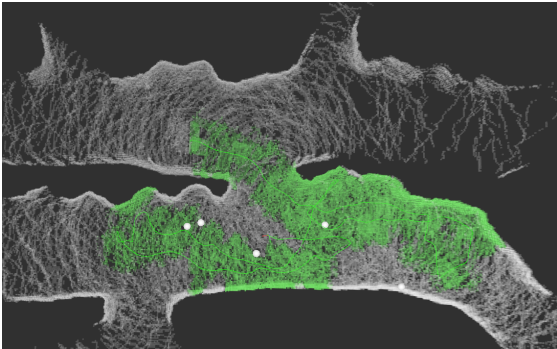


Fig. 2: The illustration of the 3D map used for exploration. The green voxels denote camera observed map, white voxels denote frontier map and white spheres denotes locations of the objects the robot detected.

The exploration policy we use is based on frontier-exploration. The occupied voxels of the frontier map are clustered into groups of neighboring voxels. Then the centroids of these clusters are extracted as the frontier points. Once the frontiers are computed, we sample a set of viewpoints within a cylinder centered at each clustered centroids. These viewpoints are 3D positions which serve as goals for the planners. The planning goals are selected based on the Euclidean distance from the robot to the candidate viewpoints, and the direction of the robot’s movement. We use a heretical planner which consists of local planner and global planner. The global planner is a RRT planner and the local planner is based on a trajectory library of desired motions. The details of the planning algorithms used in the exploration is described in [21].

B. Intrinsic Rewards Design

As introduced before, the interesting objects in the environment are sparse and thus it is not appropriate to completely rely on detected objects as the extrinsic reward for exploration. Thus we would design some other intrinsic rewards. Our major goal is to gain as much visual information coverage and Lidar coverage as possible. At the same time, we would like the robot avoid visited regions while exploring the environment.

It would be ideal that the robot can continuously gather new information. In that sense, the quantity of the information would increase over a time period. Thus intuitively, we

can compute the intrinsic rewards based on the difference between the information quantity at current time step with that at a past time step. The information quantity can be directly represented as the number of voxels of the map, either camera observed map or frontier map. Thus we proposed the following intrinsic rewards:

Camera visual coverage gain CG at time step t which is described as

$$CG(t) = C(t) - C(t - \Delta t) \quad (1)$$

Lidar frontier map gain LG at time step t which is described as

$$LG(t) = L(t) - L(t - \Delta t) \quad (2)$$

Here $C(t)$ and $L(t)$ denote voxel number of camera observed map and voxel number of Lidar frontier map, respectively. Δt denotes the time interval to compute the visual and Lidar gains.

Although the extrinsic rewards such as objects are sparse and do not exist in many circumstances, we will still include extrinsic rewards such as number of new objects detected. Hence we add a third component OG of the overall rewards described as following:

$$OG(t) = O(t) - O(t - \Delta t) \quad (3)$$

Thus the final overall reward is denoted as a weighted summation of the components described above.

$$R(t) = aCG(t) + bLG(t) + cOG(t) \quad (4)$$

where a , b and c denotes the weight factors for different types of intrinsic or extrinsic rewards. We sign equal weights in our experiment.

Based on our designed rewards, the state value function at time step t given the exploration policy π is thus formulated as the expected return starting from state s :

$$\begin{aligned} V_\pi(s) &= \mathbb{E}_{\pi,p} [G_t | s_t = s] \\ &= \mathbb{E}_{\pi,p} \left[\sum_{i=0}^{T-1} \gamma^i R(t+i+1) | s_t = s \right] \end{aligned} \quad (5)$$

where T denotes the planning horizon, γ denotes the discounting factor, G_t and s_t represent the return and state at time step t , respectively. We will discuss about the state representation in the next section.

Note that the intrinsic reward we designed here is actually not used in the original exploration policy. Thus the policy is not yet optimal for the state value function described in Equation 5. The purpose we are evaluating this exploration policy described in Section IV.A is that we can use this estimated value function for future exploration. In the new exploration environment, this learned value function can serve as an import heuristic for the graph searching algorithm used in the exploration policy.

C. State Representation

As described in the PROBLEM FORMULATION section, our state space \mathcal{S} is continuous and can be represented by various of sensors. The information which may have an impact on the state are listed as:

- Robot locations at given time steps.
- Topology of the environment around the robot location.
- Camera observed map and frontier map coverage at given time step.
- Visual information of the environment observed from the on-board camera.

The cropped local map centered around the robot location is a 3D occupancy grid map. However, feeding a 3D voxel map to a deep neural network-based function approximator is fairly computational expensive. Considering the constraints of the computation, we could use the 2D projection of the 3D occupancy map (including both camera observed map and frontier map) which can also well preserve the shape of the local map as well as the camera coverage and frontier map information. This information is crucial for the intermediate intrinsic rewards and the value function for that state.

The visual information can be directed obtained from the RGB image sequences captured from the on-board camera. We crop the image as a square to feed into the function approximator more easily. One example of the state representation is shown as Fig. 3.

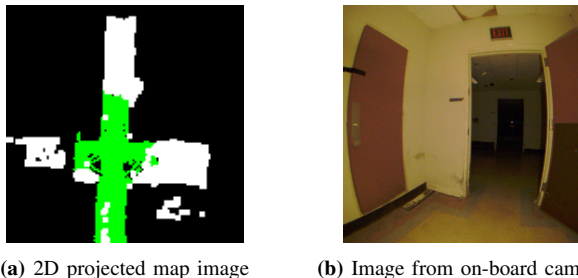


Fig. 3: Each state is represented as one 2D projected map image from the 3D voxel map built by Lidar, and one RGB image from the on-board camera. In sub-figure (a), the white pixels denote projected frontier map and the green pixels are camera observed map.

D. Value Function Approximation

1) Offline training and online learning:

Next we will introduce the detailed method of value function approximation. The parameters of the function approximator is denoted as θ . Thus the general prediction objective function we try to optimize is formulated as,

$$J(\theta) = \sum_{s \in \mathcal{S}} [V_{\pi}(s) - \hat{V}(s, \theta)]^2 \quad (6)$$

where $V_{\pi}(s)$ and $\hat{V}(s, \theta)$ denote the true value function following policy π and predicted value function, respectively.

In the training stage, we adopt Monte-Carlo (MC) method for value function approximation. Thus the target value function given policy π is approximated by the return G

of each training episode. Thus the updating procedure of the function approximator parameters is shown as,

$$\theta = \theta + \eta [G_t - \hat{V}(\phi(s), \theta)] \nabla_{\theta} \hat{V}(\phi(s), \theta) \quad (7)$$

where η denotes the learning rate in gradient-based optimization algorithm and $\phi(s)$ denotes the representation of the state, which consists of camera image and the 2D projection of the voxel map.

In the testing phase, a naive approach would be predicting the value function with frozen network parameters. However, the online testing phase is pretty similar to the online training phase of those value function approximation methods or value-based control methods [23] [24] [25]. In online value function learning, it is a good idea to exploit Temporal Difference (TD) learning without waiting the end of the current exploration episode as in the case of the offline MC training.

The bootstrapping of TD learning gives us an extra opportunity to correct and improve the value function prediction in testing phase recursively. We repeatedly apply a modified Bellman backup operator \mathcal{B} and get the recursive relationship of the state value function at time step t and $t + 1$.

$$\mathcal{B}V(s_t) = R(t) + \gamma \mathbb{E}_{\pi, p}[V(s_{t+1})] \quad (8)$$

Thus, we use semi-gradient TD(0) in testing stage to further update the parameters θ of the value function approximator. Thus the parameters updating in testing is shown as the following equations,

$$\begin{aligned} \theta &= \theta + \eta [R(t) + \gamma \hat{V}(\phi(s_{t+1}), \theta) - \hat{V}(\phi(s_t), \theta)] \nabla_{\theta} \hat{V}(\phi(s_t), \theta) \\ &= \theta + \eta [\mathcal{B}\hat{V}(\phi(s_t), \theta) - \hat{V}(\phi(s_t), \theta)] \nabla_{\theta} \hat{V}(\phi(s_t), \theta) \end{aligned} \quad (9)$$

where s_{t+1} denotes the state after executing the action a_t from the exploration policy $\pi(a_t | s_t)$. The state transition is governed by a unknown state transition model $p(s_{t+1} | s_t, a_t)$.

2) Dealing with over-estimation:

Value function estimation, either state value function or action value function, are susceptible to the problem of overestimation due to distribution shift and function approximation errors [12] [10], hence the estimated value function are expected to be larger than the real value function,

$$\mathbb{E}[\hat{V}(\phi(s), \theta)] \geq \mathbb{E}[V_{\pi}(s)], \forall s \in \mathcal{S} \quad (10)$$

We also observe a fairly extent of over-estimation of value function. Thus inspired by the solution in [12], we propose to train several copies of value function networks and use the minimum prediction from these networks. The weights of these networks are denoted as $\theta_1, \theta_2, \dots, \theta_{N_V-1}$. N_V denotes the number of value function. In our approach, we choose $N_V = 2$. All of these copies of value network will be trained offline and learn online in the same way as shown in Equation 7 and 9. During online learning and testing, the estimated value function is the minimum value obtained from each these value networks:

$$\hat{V}(\phi(s), \theta) = \min_{\theta_i} \hat{V}(\phi(s), \theta_i) \quad (11)$$

3) Value network structure:

Next we introduce more details of the function approximator. We use two encoders to encode the features of the camera image and 2D projected image. The encoded features are concatenated and then passed to a Multi-layer Perceptron (MLP) layers to get the final state value function prediction. For the sake of less computational burden, we apply MobileNet-V3-Small [26] model for both camera image encoder and map state image encoder. The network structure as well as the generation of state representation is illustrated as in Fig. 4.

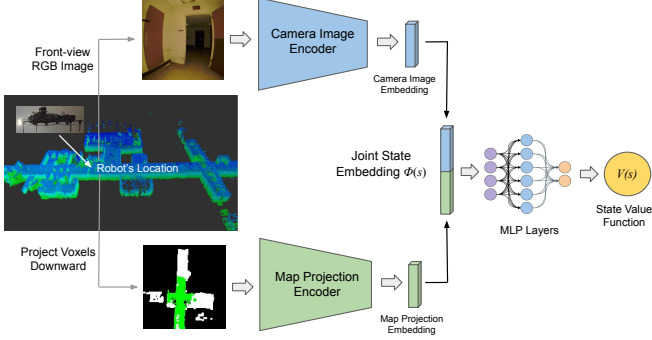


Fig. 4: Illustration of the network structure. The camera image and map projection image are sent to the encoders in parallel and then aggregated together to obtain the state value function. Note that state value function at each time step is a scalar thus the output size of the network is 1.

4) Overall algorithm:

After going through the major procedures of offline training and online learning, we present the overall algorithm illustration depicted in Fig. 5. Our value function learning algorithm consists of two major parts. The first one is the offline MC training described in Equation 7. The second step is online TD learning described as in Equation 9. The value function is trained and then online-learned to provide a feedback regarding how valuable the current state is for the robot.

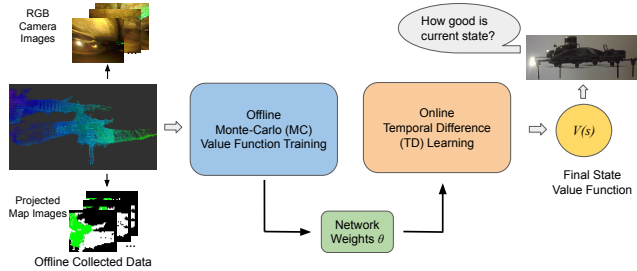


Fig. 5: Illustration of the value function approximation algorithm. First we collect datasets which are then processed to get the camera image and projected map image. Then we feed this data to the function approximator described in Fig. 4 and perform offline MC learning. After offline training, the network weights are ready to deploy for online value function estimation. However we perform one addition online TD learn step and get the final value function for the robot to determine how good the current state is.

The full value function approximation algorithms are then presented as in Algorithm 1 and 2. Algorithm 1 describes offline training with MC and Algorithm 2 describes online TD learning and testing. Please note that the notations used in these two algorithms are slightly different, e.g. network weights θ for training and θ' for testing, dataset \mathcal{D}_{tr} and \mathcal{D}_{te} , etc. Here we use double value network and in online learning phase, we use the minimum value as the final estimated value function.

Algorithm 1: Offline Training with MC

Input: State representation $\phi(s)$: camera image and cropped map

Input: Training trajectories dataset:

$$\mathcal{D}_{tr} = \{\xi_1, \xi_2, \dots, \xi_M\}$$

Output: Learned value function:

$$\hat{V}(s, \theta_1), \hat{V}(s, \theta_2), \forall s \in \mathcal{S}$$

```

1 Initialize value networks weights  $\theta_1, \theta_2$ 
2 for each training epoch do
3   for  $\xi_i \in \mathcal{D}$  do
4      $T = \text{length of } \xi_i$ 
5     for  $t = 0, 1, \dots, T - 1$  do
6       Compute return as:
7          $G_t = \sum_{i=0}^T \gamma^i R(t + i + 1)$ 
8       Update parameters as :
9          $\theta_i = \theta_i +$ 
10         $\eta [G_t - \hat{V}(\phi(s_t), \theta_i)] \nabla_{\theta_i} \hat{V}(\phi(s_t), \theta_i)$ 
11         $\forall i \in \{1, 2\}$ 
12    end
13  end

```

Algorithm 2: Online TD learning and Testing

Input: State representation $\phi(s)$: camera image and cropped map

Input: Pre-trained network weights: θ_1, θ_2

Input: Testing Trajectories data $\mathcal{D}_{te} = \{\xi\}$

Output: Estimated value function $\hat{V}(s, \theta')$

```

1 Initialize online network weights  $\theta'_1 = \theta_1, \theta'_2 = \theta_2$ 
2  $T = \text{length of } \xi$ 
3 for  $t = 0, 1, \dots, T - 1$  do
4   Receive state observation  $o_s(t)$ 
5   Receive reward  $R(t)$  following  $\pi(a_t|s_t)$ 
6   Transit to next state  $s_{t+1}$  following  $\pi$  and
7    $p(s_{t+1}|s_t, a_t)$ 
8   Online update parameters as:
9    $\theta'_i = \theta'_i +$ 
10   $\eta [\mathcal{B}\hat{V}(\phi(s_t), \theta'_i) - \hat{V}(\phi(s_t), \theta'_i)] \nabla_{\theta'_i} \hat{V}(\phi(s_t), \theta'_i)$ 
11   $\forall i \in \{1, 2\}$ 
12   $\hat{V}(\phi(s_t), \theta'_i) = \text{argmin}_{\theta'_i} \hat{V}(\phi(s), \theta'_i)$ 
13 end

```

V. EXPERIMENTS

In this section, we first introduce the data collection, including the drone platform we used to collect the data, as well as the environments where data is collected. Then we present the experiment results, in both qualitative and quantitative forms.

A. Data Collection

The drone we use for exploration and data collection is a customized quad-rotor. It is equipped with Velodyne (VLP-16) Puck Lite Lidar, Xsens MTi-200-VRU-2A8G4 IMU, Intel Realsense L515, UEye UI-3241LE-M/C RGB Camera and some wireless modules. The drone platform and relevant sensors is shown in Fig. 6.



Fig. 6: The data collection platform. This drone is equipped with a LiDAR, IMU, RGB cameras and wireless communication. The Realsense depth cameras are installed pointing up and down and are not used in this work.

The drone explores several subterranean and urban environments, including two indoor environments: a auditorium corridor and a large open room. These two indoor environments are similar to those in the DARPA Subterranean Urban Challenge [21]. We also explore one abandoned limestone mine and one natural cave. A more detailed description about these environments is shown in the following table.

Environment category	Descriptions
Auditorium corridor	structured urban indoor environment
Large open room	structured urban indoor environment
Limestone mine	long distance, wide open tunnels
Natural cave	unstructured, narrow

TABLE I: Description of the environments where data are collected

In Fig. 7 we show the snapshots of these environments. We show the RGB image captured by the on-board camera in the corners of each sub-figure, as well as the 3D occupancy grid map built by the Lidar during exploration.

B. Qualitative Results

Fig. 8 shows the qualitative value function predictions of each location the robot visited. Note here the locations cannot fully represent the state of that particular time step at which the robot is located at. We use locations to illustration the

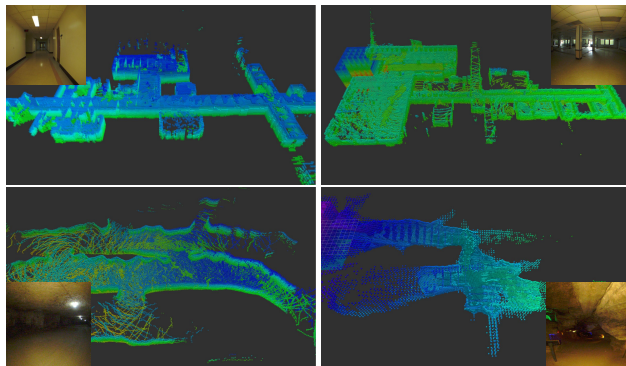


Fig. 7: Snapshots of the environments where data are collected. Here we show the sample images captured during exploration as well as the 3D reconstructed occupancy grid map. From left to right and top to bottom: Auditorium corridor, Large open room, Limestone mine and Natural cave.

relationships of the state value function at the entire map. Each location is colored to illustrate the level of the value functions. The whole locations presented in this figure can depict the overall trajectory the robot traverses. The results are obtained using double value networks scheme and TD online learning.

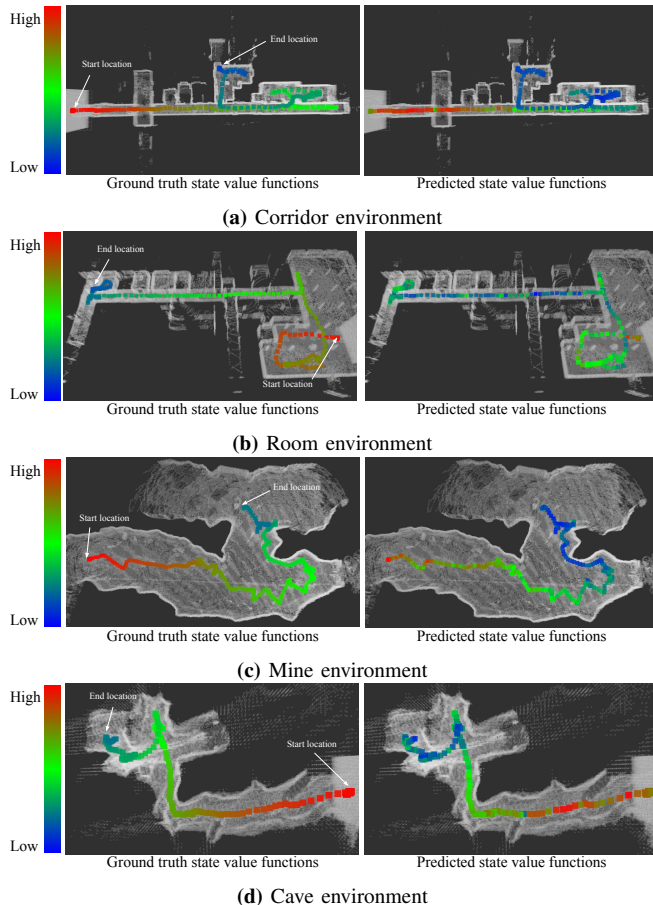


Fig. 8: Qualitative illustrations of the predicted value functions and ground truth value functions in different testing environments. Here we also label the starting and ending location of the exploration.

Environment	Normalized RMSE (lower the better)				R2 Score (higher the better)			
	Sg. w/o TD (baseline)	Sg. w/ TD (ours)	Db. w/o TD (ours)	Db. w/ TD (ours)	Sg. w/o TD (baseline)	Sg. w/ TD (ours)	Db. w/o TD (ours)	Db. w/ TD (ours)
Corridor	0.162±0.017	0.145±0.002	0.143±0.000	0.129±0.004	0.765±0.051	0.812±0.004	0.818±0.001	0.853±0.010
Room	0.261±0.001	0.314±0.073	0.258±0.000	0.213±0.002	0.318±0.005	-0.041±0.421	0.333±0.001	0.543±0.008
Mine	0.250±0.004	0.241±0.011	0.261±0.001	0.253±0.005	0.330±0.023	0.376±0.054	0.271±0.005	0.311±0.028
Cave	0.159±0.016	0.165±0.021	0.155±0.000	0.164±0.002	0.712±0.054	0.688±0.074	0.727±0.001	0.695±0.006

TABLE II: Value function prediction evaluated by NRMSE and R2 Score. Here we compare results with and without using TD learning, and the results of the single value net (Sg.) and double value net (Db.). Each entry contains the mean and std of 3 trials. We use single network without online TD learning as our baseline. We can see that our methods outperform baseline by a large margin.

C. Quantitative Results

We evaluate our value function prediction results based on the following evaluation metrics:

1) Normalized RMSE (NRMSE). Based on RMSE, We normalize it as the following:

$$\text{NRMSE} = \frac{\text{RMSE}}{V_{\pi}(s_t)_{\max} - V_{\pi}(s_t)_{\min}}, \forall t \in [0, T-1] \quad (12)$$

2) Coefficient of Determination (R2 score), which is used to measure the correlation of the predicted value function and ground truth value function. The definition of R2 score is described as in Equation 13. The highest value of R2 score is 1.

$$R^2 = 1 - \frac{\sum_{t=0}^{T-1} [\hat{V}(s_t) - v_{\pi}(s_t)]^2}{\sum_{t=0}^{T-1} [\hat{V}(s_t) - \bar{\hat{V}}(s_t)]^2} \quad (13)$$

where $\bar{\hat{V}}(s_t)$ is averaged prediction, hence

$$\bar{\hat{V}}(s_t) = \frac{1}{T} \sum_{t=0}^{T-1} \hat{V}(s_t) \quad (14)$$

Table II shows the evaluation results measured by Normalized RMSE and R2 score. Here we show results with online TD learning and without online TD learning, as well as results with and without double value networks. Since there are no prior works for this particular problem, we will take the method without using online TD learning and with just single value network as the baseline method. Our proposed methods outperform the baseline by large margin.

The following Fig. 9 show the predicted value function and ground truth value function over time. We run 3 independent testings and the mean and standard deviation (std) of the predicted value functions are shown in the curves. The left columns shows the results with single value network and with TD learning, the right columns shows the results with double value networks and with TD learning. In the vertical axis, the left part is the value function and the right part the percentage of exploration. Here the percentage of exploration is defined as the voxel number of the camera observed map N_{CM} over the voxel number of the global map N_{GM} .

$$\varphi_{\text{Explore}} = \frac{N_{CM}}{N_{GM}} \quad (15)$$

As shown in the figures, we can observe that as the exploration continues, the value function will decrease as

we expected. Since the closer we reach the end of the exploration, the newly explored area will shrink. We can also observe that the predicted value function tends to have over-estimation at the end of the episodes. By applying double value networks, the over-estimation problem is mitigated.

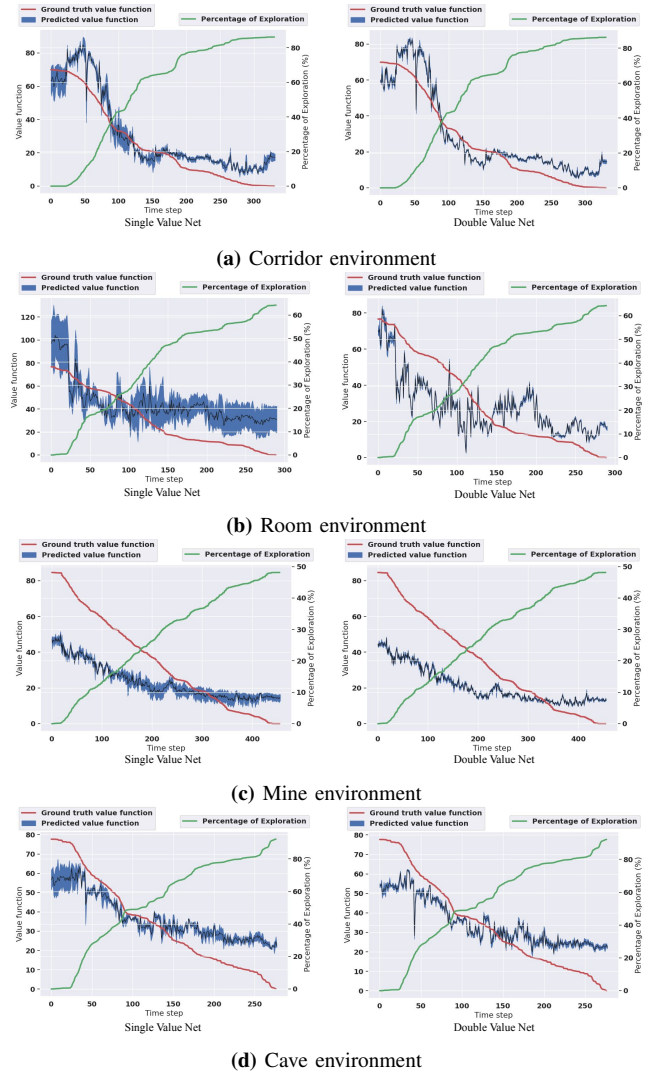


Fig. 9: Predicted value function, ground truth value function, and the percentage of exploration over time step. The left column shows the prediction with single value network and the right column shows prediction with double value network. We can observe that the variance is much smaller and the overestimation problem is alleviated, in the results with double value net.

In some cases, we need to explore a completely new environment without collecting any data in that environment. Thus we would also like to show the results across different environments, i.e. training in one environment and testing in another environment. Table III shows the evaluation results across environments. All the results are obtained with online TD learning and double value net.

Tr. \ Te.	Corridor	Room	Mine	Cave				
Corridor	0.129	0.853	0.374	-0.406	0.407	-0.775	0.379	-0.626
Room	0.270	0.352	0.213	0.543	0.381	-0.553	0.264	0.212
Mine	0.411	-0.500	0.275	0.240	0.253	0.311	0.333	-0.251
Cave	0.275	0.327	0.333	-0.113	0.369	-0.462	0.164	0.695

TABLE III: Evaluation of value function approximation across different environments. Environments listed vertically are training environments (Tr.) and those listed horizontally are testing environments (Te.). Here in each entry, the left one shows the mean NRMSE and the right one shows the mean R2 score.

It is not surprising that the diagonal entries have the best results. The value function approximator performs poorly across different environments. One interesting point to notice is that when training on room environment and testing on corridor environment, the result has relatively high R2 score and low NRMSE, this is due to the similarity of these two environments.

VI. CONCLUSIONS AND FUTURE WORK

In this paper, we present a method which approximates the state value function given previously collected data. Our method consists of offline Monte-Carlo (MC) training and online Temporal Difference (TD) learning. In order to deal with the environments with sparse reward, we proposed several intrinsic rewards to encourage exploration. To mitigate the overestimation of value function, we propose to use double value network strategy. We test our method on various challenging subterranean and urban environments. Our method outperforms the baseline method by a large margin. The experimental results shows that our proposed method can indeed generalize when testing in a new, similar environment, which means the value function can successfully transfer to a new testing environment. In the future, we plan to incorporate this value function prediction with exploration policy to improve the performance of exploration.

REFERENCES

- [1] F. Bourgault, A.A. Makarenko, S.B. Williams, B. Grocholsky, and H.F. Durrant-Whyte. Information based adaptive robotic exploration. In *IEEE/RSJ International Conference on Intelligent Robots and Systems*, 2002. 1, 2
- [2] Brian Yamauchi. A frontier-based approach for autonomous exploration brian yamauchi. In *IEEE International Symposium on Computational Intelligence in Robotics and Automation*, 1997. 1, 2
- [3] Ian Osband, Charles Blundell, Alexander Pritzel, and Benjamin Van Roy. Deep exploration via bootstrapped dqn. In *Advances in Neural Information Processing Systems*, 2016. 1

- [4] Deepak Pathak, Pulkit Agrawal, Alexei A. Efros, and Trevor Darrell. Curiosity-driven exploration by self-supervised prediction. In *International Conference on Machine Learning*, 2017. 1, 2
- [5] Marc Bellemare, Sriram Srinivasan, Georg Ostrovski, Tom Schaul, David Saxton, and Remi Munos. Unifying count-based exploration and intrinsic motivation. In *Advances in Neural Information Processing Systems*, 2016. 1, 2
- [6] Adrien Ecoffet, Joost Huizinga, Joel Lehman, Kenneth O. Stanley, and Jeff Clune. First return, then explore. *Nature*, 590(6):580–586, 2021. 1
- [7] Roberta Raileanu and Tim Rocktäschel. Ride: Rewarding impact-driven exploration for procedurally-generated environments. In *ICLR*, 2020. 1, 2
- [8] Roberto Bigazzi, Federico Landi, Silvia Cascianelli, Marcella Cornia Lorenzo Baraldi, and Rita Cucchiara. Focus on impact: Indoor exploration with intrinsic motivation. In *ICRA and RAL*, 2022. 1
- [9] Sergey Levine, Aviral Kumar, George Tucker, and Justin Fu. Offline reinforcement learning: Tutorial, review, and perspectives on open problems. In *NeurIPS 2020 Tutorial*, 2020. 1, 2
- [10] Aviral Kumar, Aurick Zhou, George Tucker, and Sergey Levine. Conservative q-learning for offline reinforcement learning. In *NeurIPS*, 2020. 1, 2, 4
- [11] Simone Parisi, Victoria Dean, Deepak Pathak, and Abhinav Gupta. Interesting object, curious agent: Learning task-agnostic exploration. In *NeurIPS*, 2020. 1, 2
- [12] Scott Fujimoto, Herke van Hoof, and David Meger. Addressing function approximation error in actor-critic methods. In *Proceedings of the 35th International Conference on Machine Learning*, 2018. 1, 4
- [13] Bradley C Stadie, Sergey Levine, and Pieter Abbeel. Incentivizing exploration in reinforcement learning with deep predictive models. In *arXiv:1507.00814*, 2015. 1, 2
- [14] Sebastian Thrun, Wolfram Burgard, and Dieter Fox. *Probabilistic Robotics*. The MIT Press, 2005. 2
- [15] Fanfei Chen Shi Bai, Jinkun Wang and Brendan Englot. Information-theoretic exploration with bayesian optimization. In *IROS*, 2016. 2
- [16] Ana Batinovic, Tamara Petrovic, Frano Petric Antun Ivanovic, and Stjepan Bogdan. A multi-resolution frontier-based planner for autonomous 3d exploration. In *RAL*, 2021. 2
- [17] A. Bircher, M. Kamel, K. Alexis, H. Oleynikova, and R. Siegwart. Receding horizon “next-best-view” planner for 3d exploration. In *ICRA*, 2016. 2
- [18] Nikolay Savinov, Anton Raichuk, Raphael Marinier, Damien Vincent, Marc Pollefeys, Timothy Lillicrap, and Sylvain Gelly. Episodic curiosity through reachability. In *ICLR*, 2019. 2
- [19] Georg Ostrovski, Marc G Bellemare, Aäron van den Oord, , and Rémi Munos. Count-based exploration with neural density models. In *Proceedings of the 34th International Conference on Machine Learning*, 2017. 2
- [20] Haoran Tang, Rein Houthoofd, Davis Foote, Adam Stooke, Yan Duan, John Schulman, Filip De Turck, and Pieter Abbeel. # exploration: A study of count-based exploration for deep reinforcement learning. In *31st Conference on Neural Information Processing Systems*, 2017. 2
- [21] Sebastian Scherer and et.al. Resilient and modular subterranean exploration with a team of roving and flying robots. *Submitted to the Journal of Field Robotics*, 2021. 2, 3, 6
- [22] Richard S. Sutton and Andrew G. Barto. *Reinforcement Learning: An Introduction*, second edition. The MIT Press, 2018. 2
- [23] Volodymyr Mnih et. al. Human-level control through deep reinforcement learning. In *Nature*, 2015. 4
- [24] Timothy P. Lillicrap, Jonathan J. Hunt, Alexander Pritzel, Nicolas Heess, Tom Erez, Yuval Tassa, David Silver, and Daan Wierstra. Continuous control with deep reinforcement learning. In *ICLR*, 2016. 4
- [25] Tuomas Haarnoja, Aurick Zhou, Pieter Abbeel, and Sergey Levine. Soft actor-critic: Off-policy maximum entropy deep reinforcement learning with a stochastic actor. In *Proceedings of the 35th International Conference on Machine Learning*, pages 1861–1870, 2018. 4
- [26] Andrew Howard, Mark Sandler, Grace Chu, Liang-Chieh Chen, Bo Chen, Mingxing Tan, Weijun Wang, Yukun Zhu, Ruoming Pang, Vijay Vasudevan, Quoc V. Le, and Hartwig Adam. Searching for mobilenetv3. In *ICCV*, 2019. 5